



ELECTRICAL PROPERTIES OF Y-TYPE SUBSTITUTED CALCIUM HEXAFERRITE

S. R. Gawali¹, P. R. Moharkar², R. R. Kherani³ and K. G. Rewatkar⁴

1 Ambedkar College, Chandrapur (M.S.), India (442401)

2 C. S. College, Chandrapur (M.S.), India (442401)

3 Shri. Shivaji Science College, Rajura (M.S.), India (442905)

4 Dr. Ambedkar College, Deekshabhoomi, Nagpur (M.S.), India (440010)

Corresponding author Email : sanjaygawali500@gmail.com

Abstract:

Hexaferrites has wide applications such as permanent magnets, core of transformer, magnetic recording media and magneto-optical devices. Keeping this view, the aluminium substituted calcium hexaferrite $\text{Ca}_2\text{Zn}_2\text{Fe}_{12-x}\text{Al}_x\text{O}_{22}$ ($x = 0.5$ and 1) have been synthesized using auto-combustion method by blending metal nitrates as oxidants accompanied with fuel like urea as reducing agent. The synthesized samples were characterized using XRD and Precision Impedance Analyzer. XRD study showed that the synthesized samples were single phase Y-type hexagonal ferrites. The effect of substitution of Al^{3+} ion for Fe^{3+} ion on the unit cell parameters, density and porosity has been studied. The DC electrical conductivity was measured as a function of temperature from room temperature to 500°C using Precision Impedance Analyzer. The phenomenon of conduction was explained on the basis of a Verway hopping mechanism. The Drift mobility of the sample increases with increase in concentration of Al^{3+} ion for Fe^{3+} ion in calcium hexaferrite.

Keywords:

Y-type hexagonal ferrite, electrical conductivity, Drift mobility etc.

Introduction

1. Introduction Y-type hexagonal ferrites are known for their high uniaxial magnetocrystalline anisotropy with the easy axis of magnetization along the hexagonal c-axis and their chemical stability [1]. These materials have been used in bulk form for many applications due to their hard magnetic properties, for example, as permanent magnets. These ferrites have drawn a great interest for magnetic recording media and microwave devices [2,3]. Hexagonal ferrites show high purity, good chemical and thermal stability which would result in longer storage life of the media. The synthesis methods reported for hexagonal





ferrites are co-precipitation [4–5], hydrothermal [6–7], sol–gel [8–9], combustion [10,11], microemulsion [12], citrate precursor [13], glass crystallization [14], sonochemical [15] and mechanochemical activation [16]. The ideal method for synthesis of hexaferrite should have Energy efficient, short reaction time, ultra fine powder, facile operation, low anneal or calcine temperature, better particle size distribution, excellent chemical homogeneity and more probability of formation of single domain structure. Keeping in view of all these characteristics, the auto-combustion method is the best method for synthesis of ferrites. In current research, Y-type calcium hexaferrite has been synthesized by auto-combustion method. It is in fact a particularly simple, safe and rapid process where in main advantages are high homogeneity, high purity and time saving and ultra fine powders. In addition, the auto-combustion method gives excellent chemical homogeneity and more probability of formation of single domain structure [17].

Material and Method

2. Experimental 2.1. Sample preparations The Y-type calcium hexaferrites having the following formula $\text{Ca}_2\text{Zn}_2\text{Fe}_{12-x}\text{Al}_x\text{O}_{22}$ ($x = 0.5$ and 1) were prepared by auto-combustion method. All the chemicals used for this synthesis were of analytical grade. The stoichiometric amounts of AR grade $\text{Ca}(\text{NO}_3)_2 \cdot 4\text{H}_2\text{O}$, $\text{Zn}(\text{NO}_3)_2 \cdot 4\text{H}_2\text{O}$, $\text{Fe}(\text{NO}_3)_3 \cdot 9\text{H}_2\text{O}$, and $\text{Al}(\text{NO}_3)_3 \cdot 9\text{H}_2\text{O}$ dissolved in filtered distilled water at the temperature of 50°C , were placed in a borosil beaker. These metal nitrates were used as oxidants reactant. The fuel urea $\text{CO}(\text{NH}_2)_2$ was also dissolve in water and is used as reducing reactant to supply requisite energy to initiate exothermic reaction amongst oxidants. All these solutions were mixed together to form homogeneous aqueous solution. The homogeneous aqueous solution is then put on magnetic stirrer we obtained wet-gel. The wet-gel was heated in the digitally controlled microwave oven of 2.45GHz for 7-10 min so that its gel get burnt by self propagating combustion reaction evolving large volumes of gases and finally get converted





in homogeneous nanocrystalline brown powdered sample. The powdered sample was then further annealed by giving intermittent moderate heat treatment for further few minutes with intermediate grinding and quenching in dry air. The sample so produced was then kept in moist free air tight compartment to avoid possible air borne reactions and for the further characterization. Characterization The phase identification of samples were carried out by using a Philips X-ray diffractometer (PW-1710) and Cu-K α radiation with the wavelength $\lambda = 1.54056 \text{ \AA}$. The X-ray pattern showed the formation of a single phase of Y-type hexagonal ferrite without any impurity. The values of lattice constant 'a' and 'c', the unit cell volume (V), X-ray density ($\rho_{x\text{-ray}}$), bulk density (ρ_m) and porosity (P) were calculated by using following equations. $1/d^2 = (4(h^2+hk+k^2))/(3a^2) + 1/c^2$ (1) $V=0.8666a^2 c$ (2) Where, 'a' and 'c' are lattice constants and 'V' is the unit cell volume. As these ferrites have very high resistivity, so the precision impedance analyzer was employed to study DC electrical resistivity of the said ferrites system in the temperature range 350 K to 770 K. The DC electrical resistivity of all the samples decreases with increasing temperature in accordance with Arrhenius equation[3] $\rho = \rho_0 \exp(\Delta E / (k_B T))$ (3) Where, 'k_B' is the Boltzmann constant, 'T' is temperature and 'ΔE' is the activation energy, which is the energy needed to release an electron from the ion for a jump to neighbouring ion, giving rise to the electrical conductivity. The activation energy of the aluminium substituted calcium hexaferrites have been determined from the slope of plots of $\ln(\rho)$ versus temperature (1000/T) above and below the transition temperature (T_t). The drift mobility (μ_d) of all synthesized hexaferrite samples were calculated using the relation[4] $\mu_d = 1 / n e \rho$ (4) where, 'e' is the charge on the electron, 'ρ' is the D.C. electrical resistivity at a given temperature and 'n' is the concentration of charge carriers and can be calculated from the relation[5] $n = (N_A \rho_m / P_{Fe}) / M$ (5) where 'N_A' is the Avogadro's number, 'ρ_m' is the bulk density, 'M' is the molecular weight of the sample, 'P_{Fe}' is the number of iron atoms in the chemical formula.





Result and Discussion

3. Results and discussion 3.1. XRD analysis The XRD patterns of the samples are shown in Fig 1. The crystallographic data are tabulated in Table 1 and 2. The data is analyzed by using computer software PCPDF Win, Powder-X and Full proof Suite. By comparing the patterns with JCPDS, the phases in the different samples are determined. It is being observed that most of the hexagonal grains are of same size. Using 2θ , observed d values and intensity calculations, d -values is recalculated and $(h k l)$ planes are finalized. The lattice parameters a and c are found to be 5.0452 \AA and 44.2512 \AA for samples. The XRD pattern confirms the formation of single phase Y-type hexagonal ferrites. The space group of the sample is found to be $(R \bar{3}m)$. The lattice parameter 'a' and 'c' decreases with increase in the concentration of Al^{3+} ion. This is due to relatively small ionic radius of Al^{3+} (0.53 \AA) comparing to that of Fe^{3+} (0.64 \AA) for six fold coordination. As a result, the cell volume of calcium hexaferrites samples decreases after being doped with Al^{3+} ion. These results agree well to that reported by Ounnunkad and Winotai [18] and Rewatkar [19] for Co-Al substituted calcium ferrite. Similar trend of lattice parameters and cell volume was reported by Sang Won Lee [20] in La-Zn substituted Strontium ferrite.

Table 2 shows that dc electrical resistivity as well as activation energy (E) increased, while the drift mobility decreased with increasing concentration of Al^{3+} ions. The drift mobility of the samples increases abruptly above the transition temperature (



Table 1: (a) Sample $\text{Ca}_2\text{Zn}_2\text{Fe}_{11.5}\text{Al}_{0.5}\text{O}_{22}$ and (b) Sample $\text{Ca}_2\text{Zn}_2\text{Fe}_{11}\text{Al}_1\text{O}_{22}$:XRD data.

2θ	dobs (Å)	dcal (Å)	I/I _o	h	k	L
19.41	4.5807	4.9008	11	0	0	9
24.255	3.6756	3.6756	26.1	0	0	<u>12</u>
33.240	2.6998	2.6785	100	1	0	<u>13</u>
33.78	2.6078	2.5945	34.1	0	0	<u>17</u>
35.695	2.5195	2.5154	69.1	1	1	0
40.920	2.2091	2.2053	21.2	0	0	<u>20</u>
49.535	1.8432	1.8378	39.6	0	0	<u>24</u>
54.145	1.6967	1.6937	49.3	0	0	<u>26</u>
54.305	1.6921	1.6930	19.2	1	0	<u>24</u>
62.510	1.4883	1.4847	26.7	1	1	<u>24</u>
62.685	1.4846	1.4834	11.7	2	1	<u>13</u>
64.080	1.4556	1.4546	25.6	3	0	0

2θ	dobs (Å)	dcal (Å)	I/I _o	h	k	L
24.20	3.6838	3.6838	29.9	0	0	<u>12</u>
29.91	2.9918	3.1073	39.2	1	0	<u>10</u>
32.38	2.7645	2.7629	97.1	0	0	<u>16</u>
33.36	2.6713	2.6834	41.9	1	0	<u>13</u>
35.03	2.5510	2.5591	100	1	0	<u>14</u>
35.56	2.5233	2.5233	74.5	1	1	0
40.87	2.2117	2.2103	23.2	0	0	<u>20</u>
42.85	2.1240	2.1206	18.0	2	0	5
49.50	1.8443	1.8419	34	0	0	<u>24</u>
53.88	1.6980	1.6972	41	0	0	<u>26</u>
56.62	1.6281	1.6232	23.2	2	1	5
62.14	1.4961	1.4875	43.1	1	1	<u>24</u>

Table 2: Lattice constants a and c, c/a ratio and cell volume (V_{cell}) of the samples

x	Sample	a(Å)	c(Å)	c/a ratio	V_{cell} (Å) ³
0.5	$\text{Ca}_2\text{Zn}_2\text{Fe}_{11.5}\text{Al}_{0.5}\text{O}_{22}$	5.0452	44.2512	8.7719	1245.11
1.0	$\text{Ca}_2\text{Zn}_2\text{Fe}_{11}\text{Al}_1\text{O}_{22}$	5.0446	44.2056	8.7629	1244.89

Table 3: Electrical resistivity at room temperature and activation energy of aluminiumsubstituted calcium ferrite

Sample	Room Temperature Resistivity ρ (MΩ-cm)	Activation Energy ΔE (eV)		Transition Temp. T_t (°K)
		Ferri	Para	
$\text{Ca}_2\text{Zn}_2\text{Fe}_{11.5}\text{Al}_{0.5}\text{O}_{22}$	121.2	0.27	0.38	515
$\text{Ca}_2\text{Zn}_2\text{Fe}_{11}\text{Al}_1\text{O}_{22}$	159.7	0.24	0.35	413

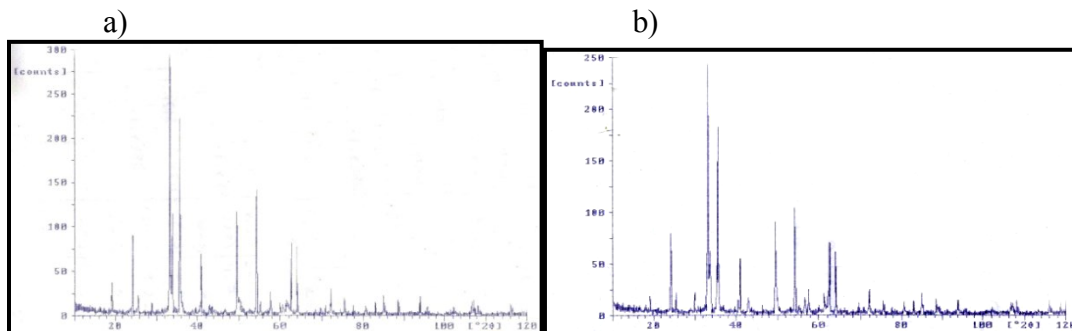


Fig. 1.(a) Sample $\text{Ca}_2\text{Zn}_2\text{Fe}_{11.5}\text{Al}_{0.5}\text{O}_{22}$ and (b) sample $\text{Ca}_2\text{Zn}_2\text{Fe}_{11}\text{Al}_1\text{O}_{22}$: X-ray diffraction spectra.

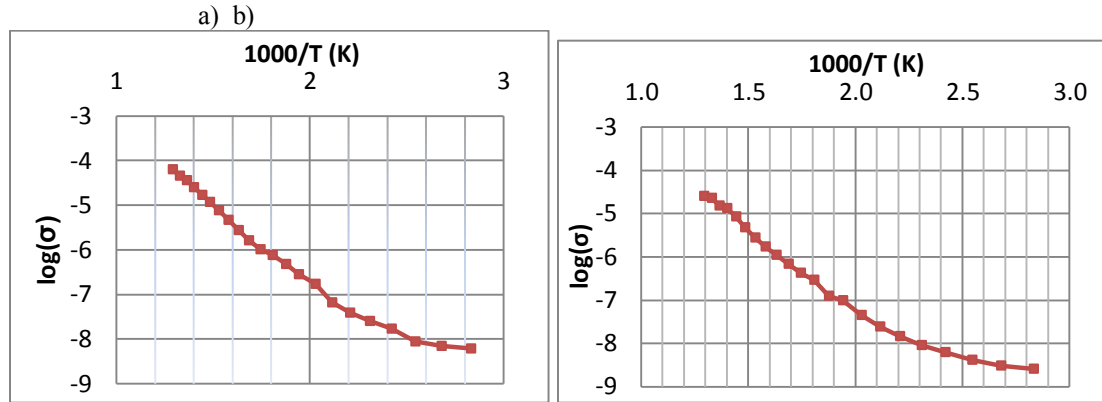


Fig. 2: Variation of $\ln(\sigma)$ with temperature ($100/T$) of sample

a) $\text{Ca}_2\text{Zn}_2\text{Fe}_{11.5}\text{Al}_{0.5}\text{O}_{22}$ and

b) $\text{Ca}_2\text{Zn}_2\text{Fe}_{11}\text{Al}_1\text{O}_{22}$

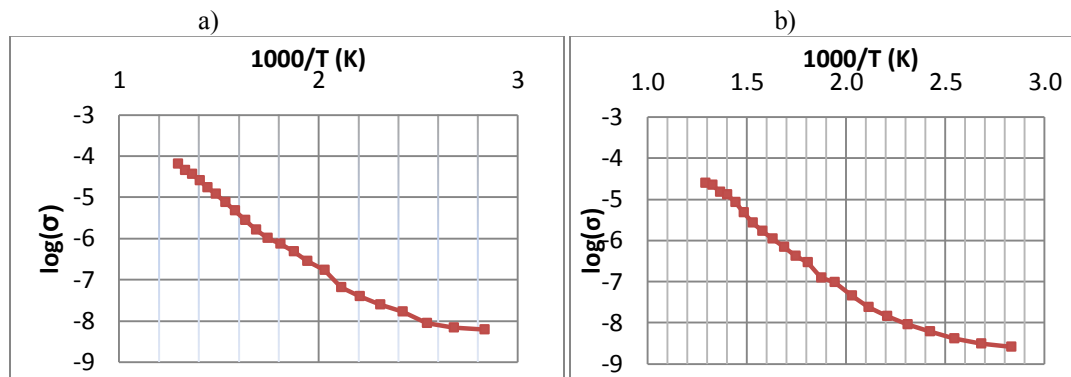


Fig. 2: Variation of $\log(\sigma)$ with temperature ($100/T$) of sample a) $\text{Ca}_2\text{Zn}_2\text{Fe}_{11.5}\text{Al}_{0.5}\text{O}_{22}$ and b) $\text{Ca}_2\text{Zn}_2\text{Fe}_{11}\text{Al}_1\text{O}_{22}$

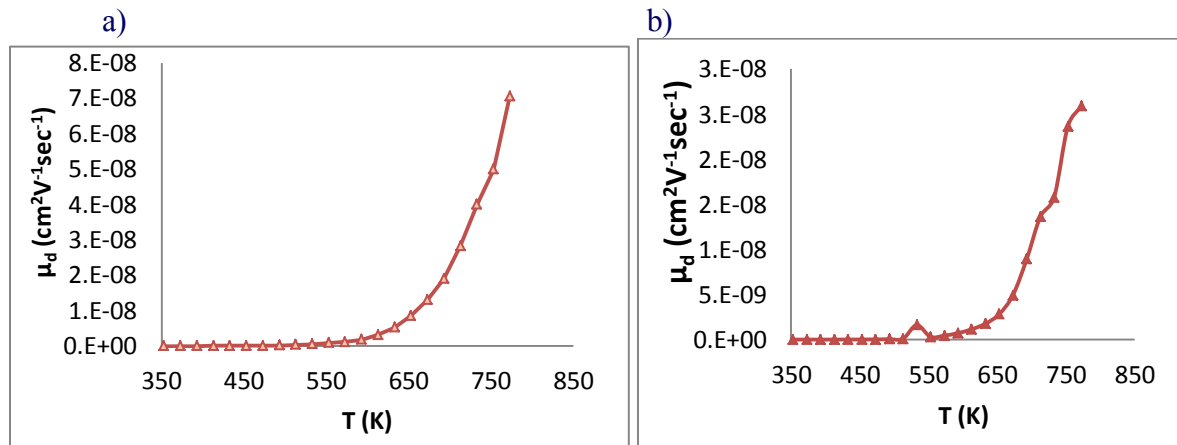


Fig. 3: Drift Mobility of samples with temperature a) $\text{Ca}_2\text{Zn}_2\text{Fe}_{11.5}\text{Al}_{0.5}\text{O}_{22}$ and b) $\text{Ca}_2\text{Zn}_2\text{Fe}_{11}\text{Al}_1\text{O}_{22}$





Conclusion

4. Conclusions The hexaferrites $\text{Ca}_2\text{Zn}_2\text{Fe}_{12-x}\text{Al}_x\text{O}_{22}$ with Al substitution were synthesized by auto-combustion method. The X-ray diffraction studies confirmed the formation of monophasic Y-type hexaferrites and the a and c values of the sample supports this confirmation. Structural studies have confirmed the space group of the samples to be $(R\bar{3}m)$. The dependence of electrical conductivity of the samples on the temperature has confirmed the semiconducting nature of sample. The conduction mechanism in calcium ferrite was explained on the basis of Verwey hopping model. The drift mobility of the sample increases with increase in temperature.

Reference

- J. Smit, H. P. J. Wijn, Les Ferrites, Dunod, Paris 1961.
- R. G. Simmons, IEEE Transactions on Magnetics 25 (1989) 4051.
- P. D. Popa, E. Rezlescu, C. Doroftei, N. Rezlescu, J. Optoelectron. Adv. Mater. 7(3), (2005)1533.
- Abdul Samee Fawzi, Adv. Appl. Sci. Research, 2 (5) (2011) 577-589.
- S. S. Khot, N. S. Shinde, B. P. Ladgaonkar, B. B. Kale, S. C. Watawe, Adv. Appl. Sci. Research, 2 (4)(2011), 460-471.
- L. Lechevallier, J. M. Le Breton, J. F. Wang, I. R. Harris, J. Magn. Magn. Mater. 269 (2004) 192.
- D. Mishra, S. Anand, R. K. Panda, R. P. Das, Mater. Chem. Phys. 86(2004) 132.
- H. Y. He, Advan. Natur. Appl. Sci., 3(2)(2009) 211.
- W. Zhong, W. Ding, N. Zhang, J. Hong, Q. Yan, Y. Du, J. Magn. Magn. Mater. 168(1997) 196.
- A. Sharma, O. Modi, G. Gupta, Adv. Appl. Sci. Research, 3(4)(2012) 2151-2158.





- S. V. Bangale, D. R. Patil, S. R. Bamane, Arch. Appl. Sci. Research, 3(5)(2011) 506-513.
- V. Pillai, P. Kumar, M. S. Multani, D. O. Shah, Colloids Surf. A: Physicochem. Eng. Aspects 80(1993) 69.
- V. K. Sankaranarayanan, D. C. Khan, J. Magn. Magn. Mater. 153(1996) 337.
- M. El-Hilo, H. Pfeiffer, K. O'Grady, W. Schuppel, E. Sinn, P. Gornert, M. Rosler, D. P. E. Dickson, R. W. Chantrell W, J. Magn. Magn. Mater. 129(1994) 339.
- K. V. P. M. Shafi, A. Gedanken, Nanostructured Mater. 12(1999) 29.
- O. Abe, M. Narita, Solid State Ionics 103(1997) 101.
- D. Lisjak, M. Drofenik, Journal of the European Ceramic Society 24 (2004) 1845.
- S. Ounnunkad , P. Winotai , J. Magn. Magn. Mater. 301 (2006) 292.
- K. G. Rewatkar , N. M. Patil , S. R. Gawali , Bull. Mater. Sci., 28(6) (2005) 585.
- Sang Won Lee, Sung Yong An, In-Bo Shim, Chul Sung Kim; J. Magn. Magn. Mater. 290 (2005) 231.
- Tawfik, Journal of Thermal Analysis, Vol. 35(1989) 141-145.

